Sensorless Manipulation Using Massively Parallel Microfabricated Actuator Arrays

Karl-Friedrich Böhringer   Bruce R. Donald

Robots & Vision Laboratory*
Department of Computer Science

Robert Mihailovich   Noel C. MacDonald

School of Electrical Engineering and
The National Nanofabrication Facility[†]

Cornell University, Ithaca, New York 14853, USA

Abstract

This paper investigates manipulation tasks with arrays of microelectromechanical structures (MEMS). We develop a geometric model for the mechanics of microactuators and a theory of sensorless, parallel manipulation, and we describe efficient algorithms for their evaluation.

The theory of limit surfaces offers a purely geometric characterization of microscale contacts between actuator and moving object, which can be used to efficiently predict the motion of the object on an actuator array. It is shown how simple actuator control strategies can be used to uniquely align a part up to symmetry without sensor feedback. This theory is applicable to a wide range of microactuator arrays. Our actuators are oscillating structures of single-crystal silicon fabricated in a IC-compatible process. Calculations show that these actuators are strong enough to levitate and move e.g. a piece of paper.

1   Introduction

A wide variety of micromechanical structures (devices typically in the μm range) has been built recently by using processing techniques known from VLSI industry. Various microsensors and microactuators have been shown to perform successfully. E.g. a single-chip air-bag sensor is commercially available [1]; video projections using an integrated, monolithic mirror array have been demonstrated recently [20]. More difficult is the fabrication of devices that can interact and actively change their environment. Problems arise from (1) unknown material properties and the lack of adequate models for mechanisms at very small scales, (2) the limited range of motion and force that can be generated with microactuators, (3) the lack of sufficient sensor information with regard to manipulation tasks, and (4) design limitations and geometric tolerances due to the fabrication process. Our work addresses in particular the first three points.

We are interested in computational tools for the design, analysis, and control of MEMS. Based on work on sensorless and near-sensorless manipulation [8, 11], we have developed geometric theories of manipulation and control for microactuator arrays, and we have developed and implemented efficient algorithms for their evaluation. Simultaneously we have designed, built, and tested microfabricated actuators (length, width $50\,\mu m$ to $200\,\mu m$) in the National Nanofabrication Facility at Cornell University. Our calculations show that arrays of these actuators are strong enough to accomplish practical manipulation tasks.

The next section briefly introduces microfabricated actuator arrays. In Section 3 we investigate geometric manipulation strategies for microactuator arrays. A model for individual actuators and their interaction with a movable object is described in section 4. Section 5 describes the design and fabrication process in some more detail. Conclusions and an outlook on future work follow in Section 6.

2   Microfabricated actuator arrays

Several kinds of devices to position small objects in the plane have been presented recently. E.g. Pister et al. [19] use an air cushion generated by micro-

fabricated nozzles to levitate objects, and move them with electrostatic forces. Takeshima and Fujita [21] introduce the concept of a *distributed micro motion system (DMMS)* that consists of an array of cooperating actuator modules. Konishi and Fujita [16] and Fujita [9] address distributed control strategies for actuator arrays. Furuhata et al. [10] have built arrays of ultrasonic microactuators. Konishi and Fujita [15] use air flow controlled by microvalves to both levitate and move objects. Ataka et al. [2] use thermobimorph cantilever beams to mimic the motion and function of cilia. Due to low friction in the air bearing, motion induced with designs [19] and [15] is fast but hard to control because of the lack of damping. Design [2] allows more control but operates at low frequencies ($\approx 1 Hz$).

Our design is closest to Furuhata's [10], with slightly larger devices and a larger range of out-of-plane motion. It combines controlled actuator-object interaction with high operation speed. It is based on microfabricated torsional resonators [17]. A torsional resonator is a rectangular grid etched out of single-crystal silicon and suspended by two rods that act as torsional springs (Figure 1a). When an AC voltage is applied between grid and adjacent electrodes, the grid oscillates at resonance frequencies in the high kHz range, the edges of the grid reaching amplitudes of several μm (Figure 1b). Our calculations have shown that the forces generated with an array of torsional resonators are large enough to levitate e.g. a piece of paper (see Section 5).
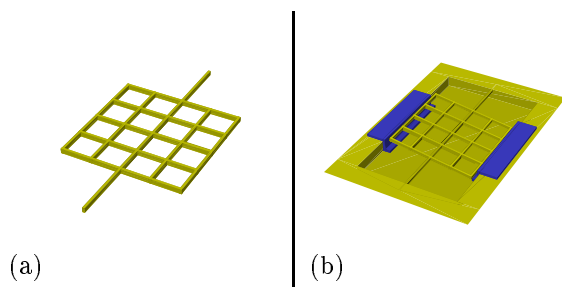

(a)   (b)

Figure 1: Torsional resonator (CAD model): (a) Resonator grid with suspending beams. (b) Resonator and electrodes (in dark color).

By introducing asymmetries into the resonator grid (such as placing the torsional rods off the center of the grid, or adding poles on one side of the grid) anisotropic lateral forces are generated, thus achieving a motion bias for the object on top of the actuator.

Each actuator can generate motion in one specific direction if it is activated, otherwise it acts as a passive frictional contact. The combination and selective activation of several actuators with different motion bias allows us to generate various motions in the plane. Figure 2 shows such a "motion pixel."

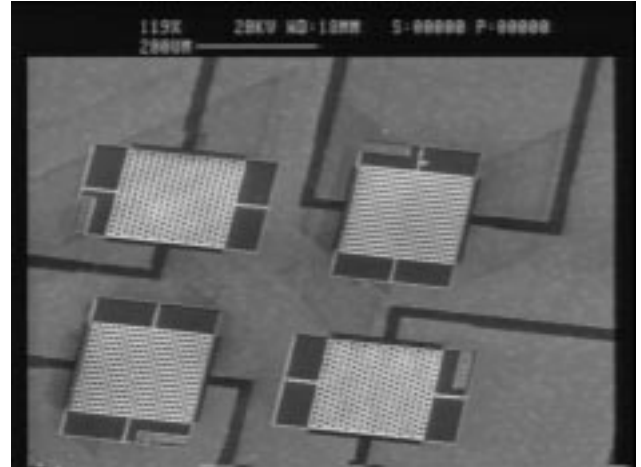Fabrication process and mechanism analysis are described in more detail in section 5.

Figure 2: Prototype motion pixel (scanning electron microscopy).

3 Macroscopic model for manipulation

In this section we develop a geometric theory of manipulation for microactuator arrays. Our ideas are based on the groundbreaking work of Erdmann and Mason [8] in the field of sensorless and near-sensorless manipulation. Their ideas have been the basis for a wide range of results, see e.g. [22, 4, 7, 14]. In this line of work on sensorless manipulation, Peshkin and Sanderson [18] have shown how to align parts on a conveyer belt with stationary fences. Goldberg [11] has given an algorithm to align parts by a sequence of grasps with a parallel-jaw gripper. In the following we show how, under reasonable assumptions, the problem of aligning a part with a microactuator array can be reduced to the alignment task with a parallel-jaw gripper, effectively using the actuator array as a two-finger gripper.

Goldberg's algorithm [11] takes the geometry of an arbitrary polygonal part P and determines its *squeeze function* $s : \mathbb{S}^1 \to \mathbb{S}^1$, where $\mathbb{S}^1$ is the set of planar orientations. The squeeze function describes the change in orientation of P when it is grasped by a parallel-jaw gripper with negligible friction. It assumes that the jaws make contact with the part simultaneously, and that the part rotates until the distance between the jaws reaches a local minimum (*squeeze grasp*). The

squeeze function can be derived from the *diameter function* $d : \mathbb{S}^1 \rightarrow \mathbb{R}$, which describes the distance between the two horizontal lines tangential to P at a particular orientation. The squeeze function maps all orientations that lie between two adjacent local maxima of the diameter function to the orientation corresponding to the intermediate local minimum (Figures 3a, b, c). Goldberg then gives an algorithm that, given a specific squeeze function, computes a sequence of grasp orientations to uniquely align P (up to symmetries) from an arbitrary initial orientation (Figure 3d). Let us summarize the results:

Theorem 1 (Goldberg [11]) *Let P be a polygon whose convex hull has n vertices. There is a sensorless control strategy $\mathcal{S}$ for a parallel-jaw gripper that aligns P up to symmetries in $O(n)$ squeeze grasps. $\mathcal{S}$ can be computed in $O(n^2)$ time.*
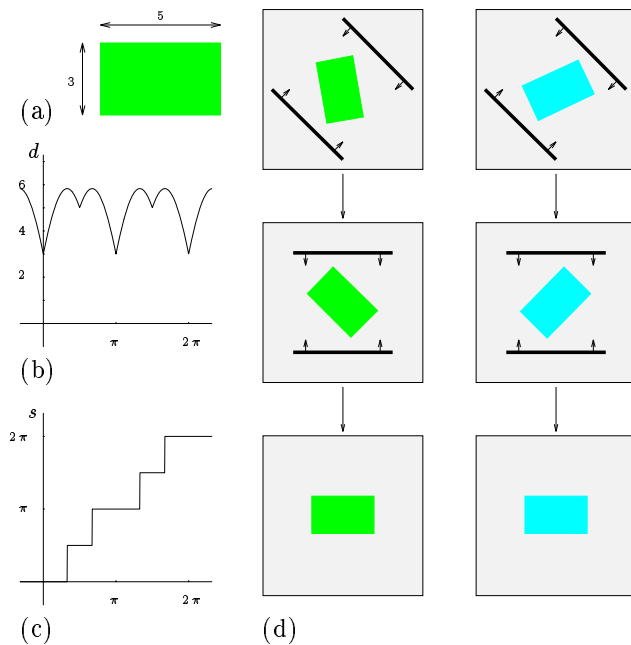

Figure 3: (a) Sample rectangle. (b) Diameter function. (c) Squeeze function. (d) Alignment strategy.

Now we show how to reduce a manipulation task with a microactuator array to an equivalent task with a parallel-jaw gripper. We make the following assumptions:

SIMPLICITY: The moving part P can be treated as a simple flat polygon.

BILATERAL SYMMETRY: We have the following simple actuator control scheme available: We can divide the array by a straight line l such that all motion pixels on either side of l push normally towards l.

DENSITY: The generated forces can be described by a two-dimensional vector field. This means that the individual microactuators are dense compared to the size of the moving part. (We will discuss later how to relax this assumption.)

We can now give a formal definition for an alignment strategy.

Definition 2 *An* alignment strategy $\mathcal{S}$ *for an actuator array is a sequence of straight lines $(l_1, \ldots, l_k)$ such that assumption* BILATERAL SYMMETRY *holds for all l_i, $1 \leq i \leq k$.*

Note that the system requires a clock that signals when enough time has elapsed for the object to reach its rest position.

Assuming quasi-static motion, a small object will move perpendicularly towards the line l and come to rest there. We are interested in the motion of an arbitrarily shaped part P. Let us call P_1, P_2 the regions of P that lie to the left and to the right of l, respectively, and C_1, C_2 their centers of gravity. In a rest position both translational and rotational forces must be in equilibrium. We get the following two conditions:

I : The areas P_1 and P_2 must be equal.

II : The vector $C_2 - C_1$ must be normal to l.

Definition 3 *A* median *of a simple polygon P is a straight line that divides P into two parts of equal size.*

Condition **I** says that l is a median of P. P has a motion component normal to l if **I** does not hold. P has a rotational motion component if **II** does not hold. P is in equilibrium (stable or metastable) iff **I** and **II** hold. Also note that because the interior of P is connected, there is a unique median for each median direction. See Figure 4 for an illustration.

For simplicity of presentation we make another assumption. This assumption will not hold in general, however it is not essential to the reduction and can be relaxed as described later. It corresponds exactly to the assumption that the parallel-jaw gripper performs pure squeeze grasps in which both jaws make contact with the part simultaneously [11].

2PHASE : The motion of P has two phases: (1) Pure translation towards l until condition **I** is satisfied. (2) Motion until condition **II** is satisfied without violating condition **I**.

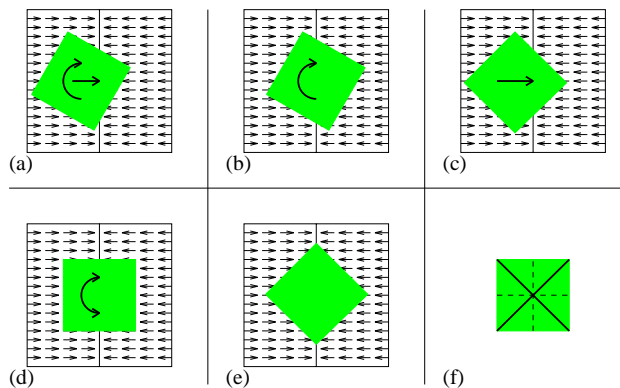The following definition is in analogy with the diameter function above:

Figure 4: Square object on actuator array: (a) **I** not satisfied, **II** not satisfied. (b) **I**, not **II**. (c) not **I**, **II**. (d) **I**, **II** (metastable). (e) **I**, **II** (stable). (f) Stable (thick) and metastable (thin) medians of square.

Definition 4 *Let ϕ be the orientation of a simple polygon P on an actuator array, and let us assume that condition* **I** *holds. The* turn function $t : \phi \to \{-1, 0, 1\}$ *describes the instantaneous rotational motion of P. $t(\phi) = 1$ if P will turn counterclockwise, $t(\phi) = -1$ if P will turn clockwise, and $t(\phi) = 0$ if P is in equilibrium.*

This definition immediately implies the following lemma:

Lemma 5 *Let P be a polygon with orientation ϕ on an actuator array such that conditions* **I** *and* **II** *hold. P is stable if $t(\phi) = 0$, $t(\phi+) \leq 0$, and $t(\phi-) \geq 0$. Otherwise P is metastable.*

Using this lemma we can identify all stable orientations, which allows us to construct the squeeze function of P in analogy to Goldberg [11]:

Lemma 6 *Let P be a simple polygonal part on an actuator array $\mathcal{A}$ such that assumptions* SIMPLICITY, BILATERAL SYMMETRY, DENSITY, *and* 2PHASE *hold. Given the turn function t of P, its corresponding squeeze function $s : \mathbb{S}^1 \to \mathbb{S}^1$ is constructed as follows:*
  1. *All stable orientations ϕ map to ϕ.*
  2. *All metastable orientations map (by convention) to the nearest right stable orientation.*
  3. *All orientations ϕ with $t(\phi) = 1$ (-1) map to the nearest right (left) stable orientation.*
Then s describes the transition of P induced by $\mathcal{A}$.

See Figures 5a, b, c for an example. We can now complete the reduction from actuator array to parallel-jaw gripper:

Theorem 7 *For a simple polygonal part P and an actuator array $\mathcal{A}$ there exists an alignment strategy*
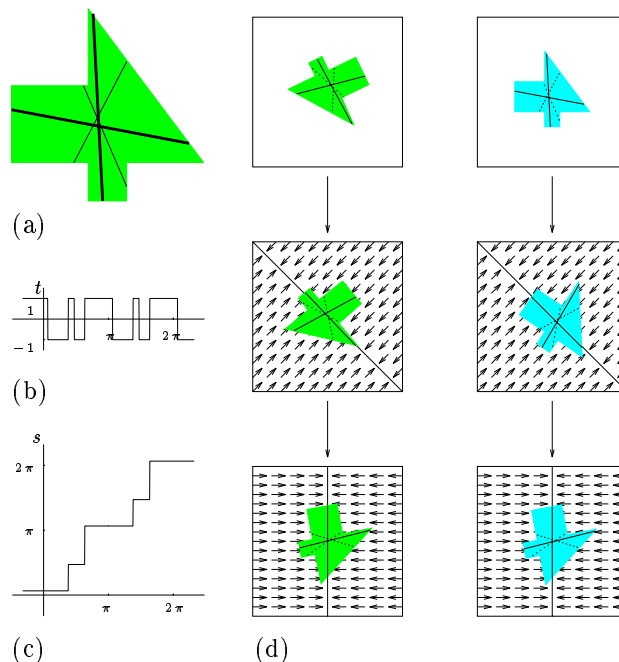

Figure 5: (a) Polygonal part. Stable (thick line) and metastable (thin line) medians are also shown. (b) Turn function. (c) Squeeze function. (d) Alignment strategy for two arbitrary initial configurations.

$\mathcal{S} = (l_1, \ldots, l_k)$ *that uniquely aligns P up to symmetries.*

Proof: We can get a formula for the turn function t of P by taking the sign of the dot product between the direction of the line l and the line connecting C_1 and C_2. Straightforward algebra shows that this product can be written as a piecewise rational function of fixed low degree, with $O(n^2)$ pieces for general simple polygons, and $O(n)$ pieces for convex polygons. From t we can construct the squeeze function s (Lemma 6) with equal complexity bounds. Then the alignment strategy $\mathcal{S}$ is obtained by using Goldberg's algorithm [11] (Theorem 1). $\square$

From the proof we obtain upper bounds for the complexity of microactuator alignment strategies:

Corollary 8 *If P is a n-gon, the algorithm runs in time $O(n^4)$ and produces a strategy $\mathcal{S} = (l_1, \ldots, l_k)$ of length $k = O(n^2)$. If P is convex the running time is $O(n^2)$ and $k = O(n)$.*

Finally let us reconsider two of the assumptions made earlier in this section. Relaxing 2PHASE corresponds to allowing *push-squeeze* grasps for the parallel-jaw gripper [11] in which one jaw pushes P before the second jaw makes contact with P. The squeeze function must be replaced by a *shift-squeeze* function which

takes combined translational and rotational motions into account. However neither the (meta-)stable orientations of P nor the complexity of the turn function will change, so the complexity of the generated strategy remains the same. Similar constructions seem possible to find reductions to conveyer belts [18] or tilting trays [8].

If we want to relax assumption DENSITY we need to model the mechanics of individual actuators and understand their interaction. Relaxing DENSITY is necessary to manipulate parts that are small relative to the actuators, which is of great interest in the field of MEMS. This is discussed in the following section.

4 Microscopic model for contacts

In this section we develop a model for the mechanics of microactuators. We make use of *limit surfaces* [12] that describe anisotropic frictional contact. We extend the model to active contacts and describe fast algorithms to compute the combined effect of many actuators.

Limit surfaces. Assume we have a part P that moves on top of the actuator array. The *limit surface* L in load space (forces F_x and F_y, moment M) fully describes the relationship between velocity v, effective applied load F_{eff}, and frictional load F_r of the moving part. It is based on the Maximum Work Inequality which is an engineering assumption commonly used when modeling friction or plasticity [12]. The Maximum Work Inequality generalizes Coulomb's friction law to anisotropic rate-independent friction. The following properties of limit surfaces are useful [12]:

1. L is a closed convex surface in load space.

2. L contains all possible frictional loads F_r on P.

3. If $v \neq 0$, F_r is on L such that $-v$ is normal to L at that point.

4. F_r is the vector inside or on L such that the length of $F_r - F_{eff}$ is minimal.

5. In the special case when the moment $M = 0$, L is a *limit curve* in $(F_x\text{-}F_y)$ load space.

See Figure 6 for examples. It follows that the inside of L contains all loads F_{eff} that can be applied to P without setting it in motion, and if $F_{eff} \neq 0$ and $v \neq 0$, F_r is determined uniquely. But note that for given v, F_r is not unique if L has a flat face with normal $-v$. Similarly for given F_r, v is not unique if L has a vertex
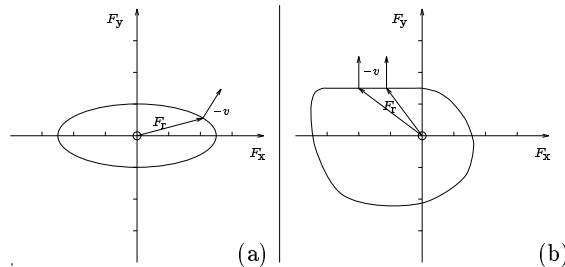

Figure 6: Limit curves: (a) $-v$ is always normal to L at F_r. (b) F_r is nonunique for specific given v.

at F_r. (This indeterminacy can be resolved by taking the inertia of P into account [12].)

Consider as an example Figure 7a. The anisotropic behavior of a wheel can be modeled with a long narrow limit curve which gives low (bearing) friction in the rolling direction and high sideways friction.
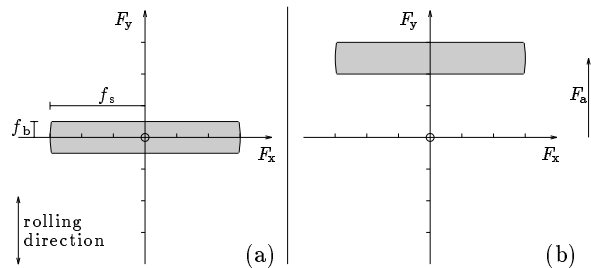

Figure 7: Limit curve of (a) passive wheel; (b) driven wheel.

Active contacts. We now extend the limit surface model to "active" contacts that apply loads to P.

Definition 9 *The* active limit surface L *in load space is the set of loads that can be applied to P without resulting in motion of P.*

This definition includes limit surfaces for passive contacts, but it allows for example to model a wheel driven by some torque τ_a. Figure 7b shows that if no additional load is applied the wheel will move in y direction, accelerated by F_a minus some bearing friction (F_a is the force accelerating the wheel with radius r such that $\tau_a = r \times F_a$). In general we get motion if the origin of load space $\mathcal{O}$ lies outside of L.

For the wheel accelerated with force F_a the limit curve simply shifts in load space by F_a. For our actuators we expect the shape of active and passive limit surface to be different because of interactions between friction and oscillation. However, because the limit surface will represent the time average over frictional contacts, we are confident that the theory of limit surfaces is a valid model.

Combining limit surfaces.

Lemma 10 *Given a rigid object P with two contact points and their respective limit surfaces L_1 and L_2, the limit surface L for P can be obtained by the Minkovski sum (convolution) $L_1 \oplus L_2$ of the two individual limit surfaces.*

If L_1 and L_2 have complexity n, L can be computed in $O(n + s)$ time, where s is the size of L, and $s = O(n^2)$ worst case.

Proof: Goyal and Ruina [12] show that limit surfaces for multiple contacts can be combined by convolution, which yields a single limit surface for the entire part. An optimal convolution algorithm with time bound $O(n + s)$ is described in Guibas and Seidel [13]. It uses a transform similar to the Fast Fourier Transform, which reduces convolution to pointwise addition. □
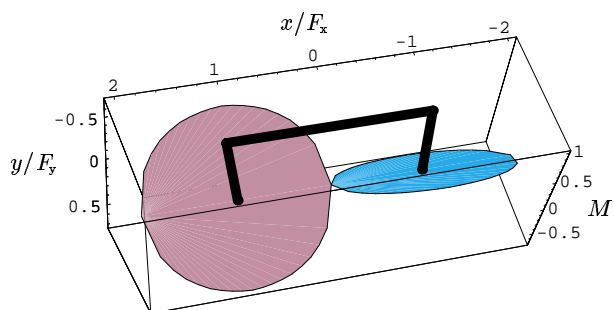

Figure 8: Bar with two point contacts at $(1, 0)$ and $(-1, 0)$, and their corresponding limit surfaces w.r.t. the center of mass $(0, 0)$.
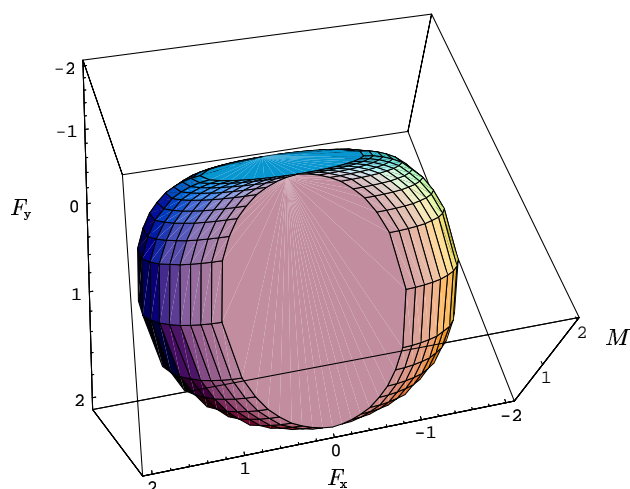

Figure 9: Combined limit surface for the object in Figure 8.

Figure 8 shows a rigid bar with two point contacts and Coulomb friction, and their corresponding limit surfaces. The individual surfaces were flat because they can generate no moment w.r.t. the contact point, but tilted because they can generate moments w.r.t.

the center of mass. The tilt angle θ can be determined by $\tan \theta = \frac{|M|}{|F|} = \frac{|r \times F|}{|F|} = |r|$, so for $|r| = 1$ we get $\theta = 45°$. Figure 9 shows the combined limit surface.

Motion prediction. Let us first consider the "upside-down" case where the actuator array "walks" on a homogeneous flat surface. The contacts and thus the limit surface L are fixed to the array frame. If $\mathcal{O}$ is inside L there will be no motion. Otherwise the generated force F is the point on L closest to $\mathcal{O}$. At that point the surface normal is parallel to F, so velocity and accelerating force are parallel. The walker will move on a straight line or a circle. This is not unexpected for a fixed actuator strategy on a homogeneous surface.

Now consider the case where the slider is on top of the actuator array. First we notice that the configuration space of the slider ($\mathbb{R}^2 \times \mathbb{S}^1$) will be partitioned into an arrangement of three-dimensional cells. In each cell a different subset of actuators is in contact with the slider.

Within each cell the contact points are fixed. Let L_0 be the limit surface for these contacts relative to $\mathcal{O}$. If we want to determine the load on the slider in configuration $s = (x, y, \phi)$ we have to transform the load by $\mathbf{T}_s = \begin{pmatrix} 1 & 0 & 0 \\ 0 & 1 & 0 \\ -y & x & 1 \end{pmatrix}$, because of the induced moment $(x, y) \times (F_x, F_y)$ around the reference point $(0, 0)$. So as the slider moves within the cell the limit surface L_s stretches along the moment axis. However the combinatorical face topology of the limit surface and its cross-section with the F_x-F_y force plane remains constant.

For a flat surface patch of L_0 given by $\mathbf{n}^T \mathbf{x} = d$, $d \geq 0$ we get an explicit formula for F_a:

$$\text{Transform: } \mathbf{n}^T \mathbf{T}_s^{-1} \mathbf{x} = d$$

$$\text{Closest point to } \mathcal{O}\text{: } F_a = \frac{d}{|\mathbf{n}_s|^2} \mathbf{n}_s$$

$$\text{with } \mathbf{n}_s = (\mathbf{n}^T \mathbf{T}_s^{-1})^T = \mathbf{T}_s^{-T} \mathbf{n}$$

More generally, if the surface patch of L_0 can be represented as a linear transform of the unit sphere, then determining F_a reduces to solving a Model Trust Region problem which has been studied in nonlinear optimization [23]. For some special cases like flat surfaces or straight lines the solution to the Model Trust Region problem yields simple formulas for F_a. Ellipsoidal surfaces require solving quartic equations. Hence for a large class of surfaces we can compute exact solutions.

We can now give a simple yet efficient motion prediction algorithm: Numerically integrate the velocities computed as described above, and update the limit surface L when a different cell in the arrangement is

entered. Each integration step can be done in constant time. Updating L is linear in the complexity of L (Lemma 10).

Motion planning. Manipulation strategies with actuator arrays require individual control for all motion pixels. The shape of the limit surface is determined by the activation pattern of the actuator array. The limit surface gives us a geometric representation of the forces and velocities generated with a specific actuator activation pattern. Though theoretically possible, there are practical limitations to plan microscopic manipulation strategies due to the combinatorial complexity and mechanical uncertainty. However, the microscopic model will prove important to analyze and verify strategies before fabrication (which is costly). It forms the link between "actuator macros" (Section 3) that predict the global behavior of manipulation strategies, and individual microfabricated mechanisms (Section 5).

5 Fabrication of actuator array

Fabrication process. The actuators are etched out of a single-crystal silicon wafer in a SCREAM (Single Crystal Reactive Etching and Metallization) process [24, 25]. The resonator grids are patterned in a photolithography step and released in a sequence of etching and oxidation steps. The metal electrodes are deposited during a self-aligning aluminum evaporation. Single beams are close to $1\,\mu m$ wide and $3\,\mu m$ high, with $\approx 3\,\mu m$ clearance. A resonator grid is typically $50 \times 50\,\mu m^2$ in size. For cleaning and improvement of levitation it is conceivable to combine the resonator with air nozzles as described in Section 2 [19]. The fabrication can be done in one to two weeks in the National Nanofabrication Facility (NNF) at Cornell University. For a more thorough discussion of design and fabrication see our companion paper [3].

Efficiency. We have analyzed an actuator of size $50 \times 50\,\mu m^2$ with clearance $h = 3\,\mu m$ using the finite element simulator COULOMB. Similar actuators are shown in Figures 1 and 2. The vertical force generated is $2.8 \cdot 10^{-7} N$ when a voltage of $50\,V$ is applied. Assuming that the resonator uses a total area of $100 \times 100\,\mu m^2$ we get $2.8 \cdot 10^{-11}\frac{N}{\mu m^2}$. This is almost two orders of magnitude higher than the specific weight of paper $80\frac{g}{m^2} \cong 8 \cdot 10^{-13}\frac{N}{\mu m^2}$. This shows that our devices are strong enough to do practical manipulation tasks. Downscaling of the devices will further improve this ratio, because the force decreases linearly with the

scaling, while the actuator density grows quadratically with decreasing scale.

Results. A wide variety of resonators has been built and tested in the NNF at Cornell University [17], yielding information on the optimal design of actuators and material properties such as stiffness, structural sturdiness, and internal stresses. A prototype of actuator arrays is currently being built.

6 Conclusions and future work

We have outlined a theory of manipulation and control for microfabricated actuator arrays that applies concepts from robotics to the field of MEMS. We believe that joint efforts in these fields are important for future MEMS of high complexity, and will prove fruitful for both areas.

The next steps of laboratory work will include the fabrication of a prototype array with a large number of microactuators, the experimental characterization of the limit surface of a microactuator, and experiments on micromanipulation to evaluate and validate our model.

The ideas presented here extend work in our group on parallel, distributed robotics [6] to massively parallel systems with similar, relatively simple individual components (DMMS [21, 16]). We are exploring how the theory of information invariants [6] could be used to automate the reductions in this paper.

Future work will include exploration of the limitations of macroscopic manipulation strategies due to the quantized forces generated by motion pixels, and the determination of quantitative error estimates. Other goals are the development and analysis of additional macroscopic strategies ("actuator macros"), in the style of Brost's "energy functions" [5] or Erdmann's "progress functions" [7], and a more detailed design and implementation of motion prediction algorithms. The low-temperature SCREAM process is compatible with conventional VLSI fabrication, which allows mechanisms and logic on one chip. This combination would make complex control strategies possible. Finally we also hope to address the case where the actuator array "walks" on a flat surface. This could conceivably lead to walking or self-assembling chips.

References

[1] Analog Devices, Inc., Norwood, MA 02062. *Introducing the ADXL50 Micromachined Accelerometer Sensor*, 1991.

[2] M. Ataka, A. Omodaka, and H. Fujita. A biomimetic micro motion system. In *Transducers — Digest Int. Conf. on Solid-State Sensors and Actuators*, pages 38–41, Pacifico, Yokohama, Japan, June 1993.

[3] K.-F. Böhringer, B. R. Donald, R. Mihailovich, and N. C. MacDonald. A theory of manipulation and control for microfabricated actuator arrays. In *IEEE Workshop on Micro Electro Mechanical Systems*, pages 102–107, Oiso, Japan, Jan. 1994.

[4] R. C. Brost. Automatic grasp planning in the presence of uncertainty. *Int. Journal of Robotics Research*, 7(1):3–17, 1988.

[5] R. C. Brost. *Analysis and Planning of Planar Manipulation Tasks*. PhD thesis, Carnegie Mellon University School of Computer Science, Pittsburgh, PA, Jan. 1991.

[6] B. R. Donald, J. Jennings, and D. Rus. Towards a theory of information invariants for cooperating autonomous mobile robots. In *International Symposium of Robotics Research*, Hidden Valley, PA, Oct. 1993.

[7] M. A. Erdmann. Randomization in robot tasks: Using dynamic programming in the space of knowledge states. *Algorithmica*, 10(2/3/4):248–291, August/September/October 1993.

[8] M. A. Erdmann and M. T. Mason. An exploration of sensorless manipulation. *IEEE Journal of Robotics and Automation*, 4(4), Aug. 1988.

[9] H. Fujita. Group work of microactuators. In *International Advanced Robot Program Workshop on Micromachine Technologies and Systems*, pages 24–31, Tokyo, Japan, Oct. 1993.

[10] T. Furuhata, T. Hirano, and H. Fujita. Array-driven ultrasonic microactuators. In *Transducers — Digest Int. Conf. on Solid-State Sensors and Actuators*, pages 1056–1059, Montreux, France, June 1991.

[11] K. Y. Goldberg. Orienting polygonal parts without sensing. *Algorithmica*, 10(2/3/4):201–225, August/September/October 1993.

[12] S. Goyal and A. Ruina. Relation between load and motion for a rigid body sliding on a planar surface with dry friction: Limit surfaces, incipient and asymptotic motion. In *WEAR*, 1988.

[13] L. J. Guibas and R. Seidel. Computing convolutions by reciprocal search. In *Proceedings of the ACM Symposium on Computational Geometry*, Urbana, IL, 1988.

[14] J. Jennings and D. Rus. Active model acquisition for near-sensorless manipulation with mobile robots. In *The IASTED International Conference on Robotics and Manufacturing*, Oxford, UK, 1993.

[15] S. Konishi and H. Fujita. A conveyance system using air flow based on the concept of distributed micro motion systems. In *Transducers — Digest Int. Conf. on Solid-State Sensors and Actuators*, pages 28–31, Pacifico, Yokohama, Japan, June 1993.

[16] S. Konishi and H. Fujita. A proposal for a conveyance system with autonomous decentralized micro modules. In *IEEE International Symposium on Autonomous Decentralized Systems*, Kawasaki, Japan, Mar. 1993.

[17] R. E. Mihailovich, Z. L. Zhang, K. A. Shaw, and N. C. MacDonald. Single-crystal silicon torsional resonators. In *IEEE Workshop on Micro Electro Mechanical Systems*, pages 155–160, Fort Lauderdale, FL, Feb. 1993.

[18] M. A. Peshkin and A. C. Sanderson. Planning robotic manipulation strategies for workpieces that slide. *IEEE Journal of Robotics and Automation*, 4(5):524–531, Oct. 1988.

[19] K. S. J. Pister, R. Fearing, and R. Howe. A planar air levitated electrostatic actuator system. In *IEEE Workshop on Micro Electro Mechanical Systems*, pages 67–71, Napa Valley, California, Feb. 1990.

[20] J. B. Sampsell. The digital micromirror device and its application to projection displays. In *Transducers — Digest Int. Conf. on Solid-State Sensors and Actuators*, pages 24–27, Pacifico, Yokohama, Japan, June 1993.

[21] N. Takeshima and H. Fujita. Design and control of systems with microactuator arrays. In *Proc. IEEE Workshop in Advanced Motion Control*, pages 219–232, Yokohama, Japan, Mar. 1990.

[22] R. H. Taylor, M. T. Mason, and K. Y. Goldberg. Sensor-based manipulation planning as a game with nature. In *International Symposium of Robotics Research*, Aug. 1987.

[23] S. A. Vavasis. *Nonlinear Optimization: Complexity Issues*, volume 8 of *International Series of Monographs on Computer Science*. Oxford University Press, New York, 1991.

[24] Z. L. Zhang and N. C. MacDonald. An RIE process for submicron, silicon electromechanical structures. *Journal of Micromechanics and Microengineering*, 2(1):31–38, Mar. 1992.

[25] Z. L. Zhang and N. C. MacDonald. Fabrication of submicron high-aspect-ratio GaAs actuators. *Journal of Microelectromechanical Systems*, 2(2):66–73, June 1993.

Historical notes and acknowledgements